expected to be more available than the metal–metal bonding pair in the $M_2S_4^{2+}$ core. The difference of 0.13 Å in the average distances of the external W–internal W atoms for $W_3S_9^{2-}$ (2.95 Å)[3] and $W_4S_{12}^{2-}$ (3.08 Å)[6] can be understood in terms of the greater facility with which MS_4^{2-} can act as an electron acceptor in the trinuclear than in the tetranuclear complex.

The average W–S(t) bond distance in $W_2S_4(edt)_2^{2-}$ is longer than the corresponding distances for either $W_4S_{12}^{2-}$ or $Mo_2S_4(edt)_2^{2-}$ by 0.05 and 0.04 Å, respectively (see Table VI). For $W_4S_{12}^{2-}$ the difference may be a consequence of the four-center bond, where removal of electron density from the internal W atoms would reduce repulsion of the terminal sulfido atoms. A related effect may be occurring in the $Mo_2S_4(edt)_2^{2-}$ case, where there are 32 fewer electrons in the molybdenum core. Additional tungsten core electrons repel multiply bonded atoms in quadruply bonded tungsten,[16] and this effect could apply to π-bonded terminal sulfido atoms. The distances of the Mo–S(t) bonds in other Mo(V) dimers[18] ligated exclusively by sulfur are shorter than the W–S(t) distances in $W_2S_4(edt)_2^{2-}$, consistent with this idea.

An alternative explanation for this difference in the M–S(t) bond lengths of these complexes is the partial occupancy of the sulfido coordination site by oxo ligands,[12] caused by partial hydrolysis of the terminal sulfido atoms. An extreme example of such a disorder was observed for $W_3S_9^{2-}$.[17] Smaller amounts of oxo contamination that are not accounted for during structure refinement would result in an artificially short determination of the M–S(t) bond length.[18a] The unavailability of infrared spectroscopic data on the samples on which the structures have been determined makes it impossible to gauge the presence or magnitude of this effect. However, in the present case, the longer W–S(t) bond makes the presence of oxo impurities very unlikely.

Conclusion

The thermal reactions of $(NH_4)_2MS_4$ (M = Mo, W) with $edtH_2$ or $abtH_2$ yield $M_2S_4^{2+}$-containing species. The reduction of M^{VI} in MS_4^{2-} to M^V may take place by internal redox rather than by reduction by the added thiols in a reaction path that does not involve $M_3S_9^{2-}$ as an intermediate. The structure of $[P(C_6H_5)_4]_2W_2S_4(edt)_2$ reveals a *syn*-$W_2S_4^{2+}$ core with dimensions very similar to those of the Mo analogue. This is the first structurally confirmed $W_2S_4^{2+}$ core in a dinuclear complex.

Registry No. $[N(C_2H_5)_4]_2Mo_2S_4(edt)_2$, 92763-40-1; $[N(C_2H_5)_4]_2Mo_2S_4(abt)_2$, 84056-94-0; $[N(C_2H_5)_4]_2W_2S_4(edt)_2$, 84051-18-3; $[N(C_2H_5)_4]_2W_2S_4(abt)_2$, 84056-96-2; $(NH_4)_2MoS_4$, 13106-76-8; $(NH_4)_2WS_4$, 13862-78-7; $[P(C_6H_5)_4]_2W_2S_4(edt)_2$, 92843-00-0.

Supplementary Material Available: Listings of calculated and observed structure factors, anisotropic thermal parameters, and derived parameters for atoms in rigid groups (35 pages). Ordering information is given on any current masthead page.

Contribution from the Anorganisch Chemisch Laboratorium, University of Amsterdam, 1018 WV Amsterdam, The Netherlands,
and Laboratoire d'Applications, Bruker Spectrospin, 67106 Wissembourg, France

^{1}H and INEPT ^{15}N and ^{109}Ag NMR Studies of the Structural and Dynamic Features in Solution of Some Silver(I) and Copper(I) Complexes with Polydentate N_4-Donor Ligands, (*R*,*S*)-1,2-(6-R-py-2-CH=N)$_2$Cy and 1,2-(6-R-py-2-CH=N)$_2$Et (Cy = Cyclohexane, Et = Ethane, R = H or Me)

GERARD C. VAN STEIN,[†] GERARD VAN KOTEN,*[†] KEES VRIEZE,[†] and CHRISTIAN BREVARD[‡]

Received January 13, 1984

The reactions of the neutral N_4-donor ligand system 1,2-(6-R-py-2-CH=N)$_2$Et (R = H or Me) with $[M(O_3SCF_3)]$ (M = Ag(I) or Cu(I)) yielded ionic complexes, consisting of a $[M_2(N_4)_2]^{2+}$ dication and $O_3SCF_3^-$ anions, which have been characterized by field-desorption mass spectrometry and INEPT ^{15}N and ^{109}Ag NMR. The dynamic behavior in solution of these $[M_2(N_4)_2]^{2+}$ dications as well as of the analogous dications with the N_4 ligands (*R*,*S*)-1,2-(6-R-py-2-CH=N)$_2$Cy (Cy = cyclohexane, R = H or Me) has been studied by ^{1}H NMR. The $[M_2(N_4)_2]^{2+}$ dications have a twofold axial symmetry. The N_4 ligands coordinate to the metal 1B centers as bis-bidentates. The metal 1B centers in the dications have similar configurations (ΔΔ or ΛΛ). Because of the presence of two inequivalent pyridine–imine H sites in these dications and the presence of $^3J(^1H-^{107,109}Ag)$ in the ^{1}H NMR spectra of the silver(I) complexes, intra- and intermolecular exchange processes could be studied in solution by ^{1}H NMR. In the spectra of the metal 1B complexes with the ethanediyl bridges a fast conformational movement was observed between two identical structures. In contrast this conformational movement does not occur in the complexes with the (*R*,*S*)-cyclohexanediyl bridging groups. The silver(I) complexes are prone to intermolecular Ag^+ exchange, which occurs with loss of $^3J(^1H-^{107,109}Ag)$. This intermolecular process may induce a configurational, $\Delta\Delta \rightleftarrows \Lambda\Lambda$, exchange process that, however, can only be observed in the ^{1}H NMR spectrum of the silver(I) complex with the (*R*,*S*)-cyclohexanediyl bridges where 6-R is H. The rates of these exchanges strongly depend on (i) the metal 1B center, M = Ag(I) or Cu(I), (ii) the 6-R substituent in the N_4 ligand, and (iii) the bridging 1,2-alkanediyl groups present. Mechanisms for these intra- and intermolecular exchange processes are proposed.

Introduction

In a previous paper[1] we reported on the solution and solid-state structures of dimeric copper(I) and corresponding silver(I) complexes with the N_4-donor ligands (*R*,*S*)-1,2-(6-R-py-2-CH=N)$_2$Cy (Cy = cyclohexane) (R = H, **1a**; R = Me, **1b**). The molecular geometry of the dication of a representative complex, $[Ag_2(\mu$-(*R*,*S*)-1,2-(py-2-CH=N)$_2$Cy)$_2](O_3SCF_3)_2$ (**2a**), is shown in Figure 1. ^{1}H and ^{13}C NMR studies revealed that these copper(I) and silver(I)

[†] University of Amsterdam.
[‡] Bruker Spectrospin.

(1) van Stein, G. C.; van Koten, G.; Vrieze, K.; Brevard, C.; Spek, A. L. *J. Am. Chem. Soc.* **1984**, *106*, 4486.

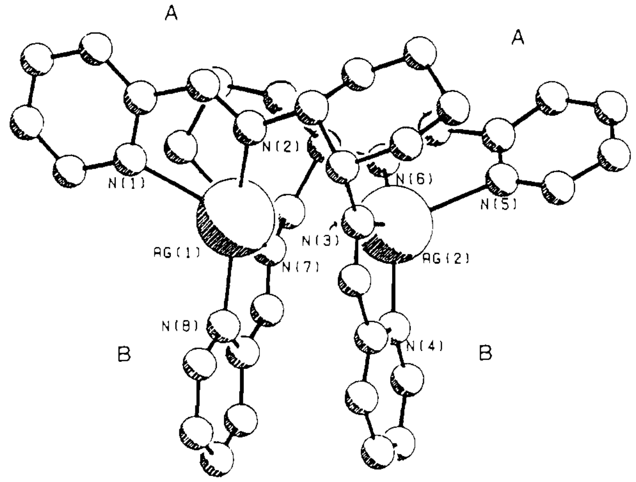

Figure 1. PLUTO drawing of the $[Ag_2(\mu\text{-}(R,S)\text{-}1,2\text{-}(py\text{-}2\text{-}CH{=}N)_2Cy)_2]^{2+}$ dication of **2a**. Hydrogen atoms are omitted for clarity (Ag(1)-N(1) = 2.455 (12) Å, Ag(1)-N(2) = 2.251 (11) Å, Ag(1)-N(7) = 2.440 (11) Å, Ag(1)-N(8) = 2.242 (11) Å, Ag(2)-N(3) = 2.430 (11) Å, Ag(2)-N(4) = 2.252 (13) Å, Ag(2)-N(5) = 2.429 (11) Å, Ag(2)-N(6) = 2.240 (12) Å).

complexes have similar structures in solution. Moreover, the ^{109}Ag and ^{15}N NMR data established that in solution the $[Ag_2(N_4)_2]^{2+}$ dications have a twofold axial symmetry and that two inequivalent pyridine–imine moieties are coordinated by the imine and pyridine N atoms to the silver(I) centers.

It is known that small alterations in the ligand skeleton of group 1B metal–polydentate ligand complexes can have a dramatic effect on the stereochemical features,[2] the stability, and the reactivity of such complexes.[3] ^1H and ^{13}C NMR spectroscopy is suited for a study of these aspects because both Cu(I) and Ag(I) are diamagnetic. Unfortunately, in the case of the copper(I) complexes only the ligand skeleton can be studied by using the NMR technique because Cu(I) itself is not a very suitable nucleus for providing high-resolution NMR information.[4] However, on the basis of our results of a NMR study of the silver(I) complex **2a**,[1] differences in solution structures of metal 1B complexes may be detectable by studying the metal sites in the silver(I) analogues with INEPT ^{109}Ag NMR.[5] If these complexes also contain polydentate nitrogen ligands, as in complex **2a**, the application of natural-abundance INEPT ^{15}N NMR can result in a more detailed picture by providing ^{15}N chemical shift data as well as the value(s) of $^3J(^1H\text{-}^{107,109}Ag)$.[1]

For this reason we have studied whether it is possible to detect by ^1H, INEPT ^{109}Ag, and natural-abundance INEPT ^{15}N NMR the stereochemical as well as the reactivity changes in the $[Ag_2(N_4)_2]^{2+}$ dications when (i) the C_2-alkanediyl group connecting the N-donor sites is changed from cyclohexanediyl, in which the two bridging C atoms have a chosen fixed configuration (*R*,*S*), to an achiral ethanediyl group and (ii) the pyridine 6-substituents, which are close to the N(pyridine)-Ag bonds, are changed from H to more bulky CH_3 groups. The purpose of this study on model compounds is to gather more information as to the effects that small but distinct changes of the conformation and configuration of polydentate ligand systems bound to metal 1B centers exert on the coordination and reactivity properties of these metal 1B sites.

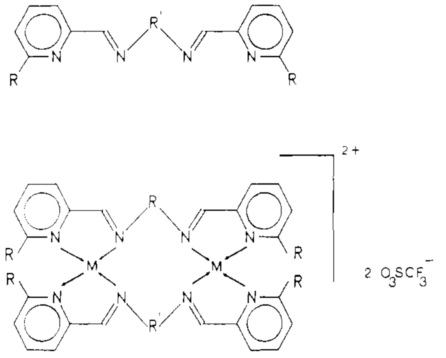

Figure 2. Schematic representation of the N_4 ligands and their silver(I) and copper(I) complexes (R = H, **a**; R = Me, **b**; R′ = (*R*,*S*)-1,2-cyclohexane (**1**), 1,2-ethane (**4**)): $[Ag_2(\mathbf{1})_2](O_3SCF_3)_2$ (**2**); $[Cu_2(\mathbf{1})_2](O_3SCF_3)_2$ (**3**); $[Ag_2(\mathbf{4})_2](O_3SCF_3)_2$ (**5**); $[Cu_2(\mathbf{4})_2](O_3SCF_3)_2$ (**6**).

In this paper we report the results of a comparative NMR study of both the silver(I) and copper(I) dications represented schematically in Figure 2.

The nature of the bridging C_2 chain appeared to be the main factor influencing the occurrence of various intramolecular H(A), H(B) site exchange processes (see Figure 1), and these were studied in detail by dynamic ^1H NMR. Furthermore, an influence of this C_2 chain on the intermolecular Ag^+ (or Cu^+) exchange process could be detected. This information, gathered on model complexes, may be of importance to understand the dynamic behavior of the metal 1B centers in copper(I)-containing enzymes.

Experimental Section

Preparation of the Compounds. The N_4 donor ligands (*R*,*S*)-1,2-(6-R-py-2-CH=N)$_2$Cy (R = H, **1a**; R = Me, **1b**) and their silver(I) complexes (**2a**,**b**) and copper(I) complexes (**3a**,**b**) have been prepared by methods described in a previous paper.[1] The ligands 1,2-(6-R-py-2-CH=N)$_2$Et (R = H, **4a**; R = Me, **4b**) were obtained by the method of Busch and Bailar.[6] Silver(I) trifluoromethanesulfonate is commercially available, and copper(I) trifluoromethanesulfonate–0.5-benzene was prepared as described in ref 7. Preparations of the metal complexes were carried out under a nitrogen atmosphere in freshly distilled solvents. Elemental analyses were carried out by the Analytical Section of the Institute for Applied Chemistry, TNO Utrecht, The Netherlands.

[Ag$_2$(μ-1,2-(6-R-py-2-CH=N)$_2$Et)$_2$](O$_3$SCF$_3$)$_2$ (R = H, 5a; R = Me, 5b). A solution of $[Ag(O_3SCF_3)]$ (2 mmol) in methanol (20 mL) was added to a solution of 1,2-(6-R-py-2-CH=N)$_2$Et (2.1 mmol) in methanol (20 mL). The reaction mixture was stirred for 15 min followed by evaporation of free solvent to afford a yellow solid. Excess free ligand was removed by washing the solid with diethyl ether (3 × 10 mL). Pale yellow crystals were obtained in an almost quantitative yield from methanolic solutions. Anal. Calcd for $C_{15}H_{14}AgF_3N_4O_3S$ (**5a**): C, 36.38; H, 2.85; F, 11.51; N, 11.31. Found: C, 36.42; H, 2.91; F, 11.42; N, 11.50. Calcd for $C_{17}H_{18}AgF_3N_4O_3S$ (**5b**): C, 39.02; H, 3.47; F, 10.89; N, 10.71. Found: C, 38.78; H, 3.56; F, 10.62; N, 10.58.

[Cu$_2$(μ-1,2-(6-R-py-2-CH=N)$_2$Et)$_2$](O$_3$SCF$_3$)$_2$ (R = H, 6a; R = Me, 6b). A solution of 1,2-(6-R-py-2-CH=N)$_2$Et (2.1 mmol) in benzene (30 mL) was slowly added to a solution of $[Cu(O_3SCF_3)]\cdot{}^1/_2C_6H_6$ (2 mmol) in benzene (30 mL). A red-brown precipitate was formed immediately. The solution was decanted and the precipitate washed with benzene (3 × 10 mL) in order to remove an excess of free ligand. Dark brown crystals were obtained in an almost quantitative yield from methanolic solutions. Anal. Calcd for $C_{15}H_{14}CuF_3N_4O_3S$ (**6a**): C, 39.96; H, 3.13; F, 12.64; N, 12.43. Found: C, 39.27; H, 3.39; F, 12.31; N, 12.51. Calcd for $C_{17}H_{18}CuF_3N_4O_3S$ (**6b**): C, 42.63; H, 3.79; F, 11.90; N, 11.70. Found: C,

---

[2] Österberg, R. *Coord. Chem. Rev.* **1974**, *12*, 309. Hathaway, B. J.; Billing, D. E. *Coord. Chem. Rev.* **1970**, *5*, 143.

[3] Karlin, K. D.; Sherman, S. E. *Inorg. Chim. Acta* **1982**, *65*, L39.

[4] ^{63}Cu or ^{65}Cu chemical shifts and $^1J(^{15}N\text{-}^{63}Cu)$, $^1J(^{15}N\text{-}^{65}Cu)$, $^nJ(^1H\text{-}^{63}Cu)$, and $^nJ(^1H\text{-}^{65}Cu)$ data are often hard to determine or even not obtainable because of the quadrupole moments of ^{63}Cu and ^{65}Cu, both having $I = {}^3/_2$: Marker, A.; Gunther, M. J. *J. Magn. Reson.* **1982**, *47*, 118 and references therein.

[5] Brevard, C.; van Stein, G. C.; van Koten, G. *J. Am. Chem. Soc.* **1981**, *103*, 6746.

[6] Busch, D. H.; Bailar, J. C., Jr. *J. Am. Chem. Soc.* **1956**, *78*, 1137.

[7] Salomon, R. G.; Kochi, J. K. *J. Am. Chem. Soc.* **1973**, *95*, 1889.

42.58; H, 4.00; F, 11.96; N, 11.70.

Physical Measurements. Infrared (IR) spectra were measured on a Perkin-Elmer 283 spectrophotometer as KBr pellets (see Table SI, deposited as supplementary material). Field desorption mass spectra were obtained with a Varian MAT 711 double-focusing mass spectrometer containing a combined EI/FI/FD ion source and coupled to a Spectro-System MAT 100 data acquisition unit.[8] The samples were loaded onto the emitter with the dipping technique.[9] FD mass spectral data are given in Table SII (deposited as supplementary material).

^{19}F NMR spectra of the new complexes **4a**, **4b**, **5a**, and **5b** were recorded on a Varian XL-100 spectrometer with $CFCl_3$ as external reference in methanol-d_4 (see Results).

Natural-abundance ^{15}N and ^{109}Ag spectra were recorded on a Bruker WM 250 spectrometer in methanol-d_4 applying the INEPT[10] polarization sequence. The procedure for obtaining the spectra has been described in a previous paper.[1] For the ^{15}N and ^{109}Ag chemical shift data $MeNO_2$ in C_6D_6 (80/20 v/v) and $AgNO_3$ (2 M in D_2O) respectively were used as external references (for ^{15}N and ^{109}Ag NMR data see Tables I and II, respectively).

^1H NMR spectra were recorded on Bruker WM 250 and WM 400 spectrometers in methanol-d_4 with tetramethylsilane (Me_4Si) as reference (Table II). Exchange rates, $1/\tau$, in the symmetrical two-site system, imine H(A), H(B), in the $[Ag_2(\mathbf{1a})_2]^{2+}$ dication of **2a** (0.032 M) with free $[Ag(O_3SCF_3)]$ (0.014 M) in methanol-d_4 have been measured (400 MHz) by spin saturation transfer (SST)[11] at eight different temperatures (see Table III) with use of the expression $1/\tau = (1/T_{1B})[(M_0/M_\infty) - 1]$. T_1 represents the spin-lattice relaxation time of the imine proton of site B, M_0 is the normal equilibrium magnetization, and M_∞ is the equilibrium magnetization of proton B after saturating the imine proton resonance of site A. T_1 values have been measured by the inversion recovery Fourier transform (IRFT) method with the well-known sequence $[180°-\tau-90°\ (FID)-T]_n$. Rates of the imine-H(A), -H(B) exchange in samples of **2a** (0.025 M) with free $[Ag(O_3SCF_3)]$ in the concentration range of 0.048–0.202 M at $T = 294$ K (250 MHz) have been obtained with use of the equation $1/\tau = (\pi/2^{1/2})(\delta\nu^2 - \delta\nu_e^2)^{1/2}$, in which $\delta\nu$ represents the separation of the imine proton resonances of the two sites, A and B, in the nonexchange region (in Hz) and $\delta\nu_e$ the observed separation of the signals in the slow exchange (see Table III).

Results

Characterization of the Complexes Having the 1,2-Ethanediyl Bridge. The only Ag(I) and Cu(I) complexes that could be obtained with the N_4-donor ligands 1,2-(6-R-py-2-CH=N)$_2$Et (R = H, **4a**; R = Me, **4b** (see Figure 2)) are $[Ag_2(\mathbf{4})_2](O_3SCF_3)_2$ (**5**) and $[Cu_2(\mathbf{4})_2](O_3SCF_3)_2$ (**6**), for which the analytical data confirms a 1/1 metal salt to ligand ratio. This parallels the observation made earlier for the synthesis of Cu(I) and Ag(I) complexes with the N_4 ligands **1a** and **1b** (containing the (*R*,*S*)-1,2-cyclohexanediyl bridge) where exclusively the 1/1 complexes (i.e. $[M_2(\mathbf{1})_2](O_3SCF_3)_2$) were formed.[1]

IR spectra of **5a,b** and **6a,b** show characteristic patterns for noncoordinating $O_3SCF_3^-$ anions with C_{3v} symmetry[1,12] (e.g. for **6a** (cm^{-1}): ν_4(E), 1264; ν_1(A1), 1032; ν_5(E)δ(SO_3), 635 (see Table SI for full data)).

The ^{19}F NMR data of the $[M_2(\mathbf{4})_2](O_3SCF_3)_2$ complexes **5** and **6** are likewise in accordance with the presence of noncoordinating $O_3SCF_3^-$ anions.[1,13] The spectra, in methanol-d_4, show for all four complexes one singlet resonance with a chemical shift of $\delta = -78.4$.[14]

Table I. INEPT (Natural Abundance) ^{15}N NMR Data[a] of the Ligands 4a and 4b and $[Ag_2(4b)_2](O_3SCF_3)_2$ (5b) and $[Cu_2(4)_2](O_3SCF_3)_2$ (6a and 6b)

	δ [$^1J(^{15}N-^{107,109}Ag)$, Hz]			
compd	^{15}N (imine)	Δ[b]	^{15}N (pyridine)	Δ
		Ligands		
4a	−47.0		−74.4	
4b	−49.6		−77.1	
		Complexes		
$[Ag_2(4b)_2]^{2+}$	−88.6 [40.9]	−39.0	−107.0 [23.9]	−29.9
$[Cu_2(4a)_2]^{2+}$	−94.0	−47.0	−110.5	−36.1
$[Cu_2(4b)_2]^{2+}$	−94.2	−44.6	−112.6	−35.5

[a] Obtained in methanol-d_4 at $T = 294$ K; see Experimental Section. [b] $\Delta = \delta(\text{complex}) - \delta(\text{ligand})$.

Field desorption mass spectra[15] (see Table SII for full data) were in agreement with the dinuclear nature of the $[M_2(\mathbf{4})_2]^{2+}$ dications.

The pure silver(I) and copper(I) complexes $[M_2(\mathbf{1})_2](O_3SCF_3)_2$ show in their ^1H NMR spectra at room temperature, as we have reported in a previous paper,[1] two pyridine–imine H patterns that correspond to two different pyridine–imine halves in the molecular structures. This situation has been confirmed for the $[Ag_2(\mathbf{1a})_2]^{2+}$ dication (see Figure 1) in the solid state. For the present complexes **5** and **6** it is important to realize that the imine proton resonances of the silver(I) complexes $[Ag_2(\mathbf{1})_2](O_3SCF_3)_2$ (**2a** and **2b**) appear as doublets due to $^3J(^1H-^{107,109}Ag)$[16] while on the imine-^{15}N and pyridine-^{15}N resonances $^1J(^{15}N-^{107,109}Ag)$ couplings[16] are also present (see Figure 4 in ref 1).

The INEPT ^{15}N NMR spectra of the silver(I) (**5b**) and copper(I) (**6a** and **6b**) complexes $[M_2(\mathbf{4})_2](O_3SCF_3)_2$ showed only one type of pyridine–imine unit, i.e. one resonance for the imine and another for the pyridine ^{15}N atoms (see Table I). This observation indicates that in contrast to the nonequivalent pyridine–imine halves in the $[M_2(\mathbf{1})_2]^{2+}$ dications those in the $[M_2(\mathbf{4})_2]^{2+}$ dications are isochronous on the ^{15}N (and ^1H) NMR time scale. For the silver(I) complex **5b** these two ^{15}N signals appeared as *doublets* of *doublets* whereas in the case of the copper(I) complexes **6a** and **6b** both signals were observed as simple doublets. ^{15}N-selective ^1H (imine) decoupling experiments proved that the low-field resonances belong to the imine-^{15}N atoms and those at higher field to the pyridine-^{15}N atoms. A $^{15}N\{^1H\}$ (BB) experiment of the silver(I) complex **5b** revealed that the small couplings of the doublets of doublets arise from $^nJ(^{15}N-^1H)$ and therefore the larger ones are due to $^1J(^{15}N-^{107,109}Ag)$.[16] The presence of $^1J(^{15}N-^{107,109}Ag)$ on both the imine- and pyridine-^{15}N resonances in the spectrum of **5b** unambiguously proves that all four N atoms of each of the two N_4 ligands are coordinating to the silver(I) centers. In the spectra of the copper(I) complexes $[Cu_2(\mathbf{4})_2](O_3SCF_3)_2$ (**6a** and **6b**) this direct evidence for N–Cu bonding is lacking.[4] However, the large chemical shifts of both the imine-*N* and the pyridine-*N* atoms relative to those found for the free ligands is a strong indication that

---

(8) Van der Greef, J.; Pinkse, F. A.; Kort, C. W. F.; Nibbering, N. M. M. *Int. J. Mass Spectrom. Ion Phys.* **1977**, *25*, 315.

(9) Wolkoff, P.; van der Greef, J.; Nibbering, N. M. M. *J. Am. Chem. Soc.* **1978**, *100*, 541.

(10) Morris, G. A.; Freeman, R. *J. Am. Chem. Soc.* **1979**, *101*, 760. Morris, G. A. *J. Am. Chem. Soc.* **1980**, *102*, 428.

(11) Mann, B. E. *J. Magn. Reson.* **1976**, *21*, 17.

(12) Dedert, P. L.; Thompson, J. S.; Ibers, J. A.; Marks, T. J. *Inorg. Chem.* **1982**, *21*, 969.

(13) Noftle, R. E.; Cady, G. H. *Inorg. Chem.* **1965**, *4*, 1010.

(14) A positive δ corresponds to a higher resonance frequency ("deshielding") with respect to the reference frequency.

(15) Beckey, H. D. "Principles of Field Ionization and Field Desorption Mass Spectrometry"; Pergamon Press: New York, 1977. Staal, L. H.; van Koten, G.; Fokkens, R. H.; Nibbering, N. M. M. *Inorg. Chim. Acta* **1981**, *50*, 205.

(16) Because of the small values of the couplings in combination with the small difference in γ values of ^{107}Ag and ^{109}Ag the respective doublets arising from $^3J(^1H-^{107}Ag)$ and $^3J(^1H-^{109}Ag)$ and from $^1J(^{15}N-^{107}Ag)$ and $^1J(^{15}N-^{109}Ag)$ are not resolved: ^{107}Ag (51.81%) and ^{109}Ag (48.18%) both have $I = {}^1/_2$ with γ values of -1.0828×10^7 and -1.2449×10^7 rad T^{-1} s^{-1}, respectively.

(17) Allerhand, A.; Gutowsky, H. S.; Jonas, J.; Meinzer, R. A. *J. Am. Chem. Soc.* **1966**, *88*, 3185.

(18) van Stein, G. C.; van Koten, G.; Spek, A. L.; Duisenberg, A. J. M.; Klop, E. A. *Inorg. Chim. Acta* **1983**, *78*, L61.

Table II. ^1H and ^{109}Ag NMR Data Obtained at 294 K in Methanol-d_4[h]

compd	site	H(im)[a]	H-3	H-4	H-5	H-6	H(6-Me)	α-H	δ^{14} $^{109}Ag\{^1H\}$ (BB)
Ligands									
1a		8.27 s	8.00 d	7.83 dd	7.40 dd	8.53 d		3.72 m	
1b		8.27 s	7.80 d	7.65 dd	7.21 d		2.48 s	3.68 m	
4a		8.36 s	7.98 d	7.86 dd	7.42 dd	8.56 d		4.04 s	
4b		8.30 s	7.77 d	7.70 dd	7.20 d		2.51 s	4.02 s	
Complexes									
$[Ag_2(1a)_2]^{2+}$	A	8.87 d[b]	7.91 d	8.10 dd	7.61 dd	8.38 d		4.21 m	+580 s
	B	8.69 d[c]	7.47 d	7.79 dd	7.32 dd	8.13 d			
$[Ag_2(1b)_2]^{2+}$	A	8.89 d[d]	7.74 d	8.01 dd	7.52 d		2.16 s	4.21 m	+612 s
	B	8.79 d[e]	7.48 d	7.69 dd	7.24 d		2.08 s		
$[Cu_2(1a)_2]^{2+}$	A	8.90 s	7.92 d	8.04 dd	7.52 dd	8.11 d		4.31 m	
	B	8.40 s	7.10 d	7.72 dd	7.46 dd	8.11 d			
$[Cu_2(1b)_2]^{2+}$	A	8.90 s	7.81 d	8.00 dd	7.50 d		2.16 s	4.34 m	+618 s
	B	8.40 s	6.97 d	7.68 dd	7.48 d		1.82 s		
$[Ag_2(4a)_2]^{2+}$		8.70 s[f]	7.64 d	7.96 dd	7.50 dd	8.32 d		4.27 s	
$[Ag_2(4b)_2]^{2+}$		8.79 d[g]	7.55 d	7.87 dd	7.46 d		2.26 s	4.30 s	
$[Cu_2(4a)_2]^{2+}$		8.67 s	7.56 d	7.99 dd	7.64 dd	8.30 d		4.31 s	
$[Cu_2(4b)_2]^{2+}$		8.57 s	7.38 d	7.86 dd	7.53 d		2.08 s	4.31 s	

[a] H(im) resonances of the silver(I) complexes appear as doublets due to $^3J(^1H-^{107,109}Ag)$. [b] $J = 9.3$ Hz. [c] $J = 6.3$ Hz. [d] $J = 10.5$ Hz. [e] $J = 7.5$ Hz. [f] $J = 8.5$ Hz ($T < 241$ K). [g] $J = 9.3$ Hz. [h] Abbreviations: s = singlet, d = doublet, dd = doublet of doublets, m = multiplet.

in the copper(I) complexes the N atoms are also coordinated to the metal centers. Because of the preference of four-coordinate metal 1B centers for tetrahedral geometries one may therefore conclude that the metal 1B complexes of the N_4 ligands with the 1,2-ethanediyl bridging group have similar dimeric $[M_2(\mathbf{4})_2](O_3SCF_3)_2$ structures in solution. As in the $[Ag_2(\mathbf{1})_2](O_3SCF_3)_2$ complexes with the N_4 ligands **1**, the ligands **4** in the $[M_2(\mathbf{4})_2](O_3SCF_3)_2$ complexes are bis-bidentate bonded (see Figure 2).

The INEPT ^{109}Ag NMR spectrum of $[Ag_2(\mathbf{4b})_2](O_3SCF_3)_2$ (294 K, methanol-d_4) shows one doublet resonance at +618 ppm,[14] which is close to the value found for the silver(I) complex $[Ag_2(\mathbf{1b})_2](O_3SCF_3)_2$ having (*R*,*S*)-1,2-cyclohexanediyl bridging groups (see Table II). The presence of only one ^{109}Ag resonance shows that also in the $[Ag_2(\mathbf{4b})_2]^{2+}$ dications there is a twofold axial symmetry present (see Discussion).

To investigate the differences in dynamic behavior and reactivity in solution of the silver(I) and copper(I) complexes $[M_2(N_4)_2](O_3SCF_3)_2$ (N_4 = (*R*,*S*)-1,2-(6-R-py-2-CH=N)$_2$Cy (**1**), 1,2-(6-R-py-2-CH=N)$_2$Et (**4**) (R = H, Me)) we have made a detailed ^1H NMR study, the results of which are presented below. The ^1H NMR data (250 MHz, room temperature) of the free ligands **1** and **4** as well as of the silver(I) and copper(I) complexes are presented in Table II. The labels A and B are used to denote the protons belonging to the nonequivalent pyridine–imine halves as observed in the spectra of the $[M_2(\mathbf{1})_2](O_3SCF_3)_2$ complexes.

Dynamic ^1H NMR Study in Methanol-d_4 of $[M_2(\mathbf{1})_2](O_3SCF_3)_2$ (1 = (*R*,*S*)-1,2-(6-R-py-2-CH=N)$_2$Cy; R = H (a), R = Me (b)). Pure $[Ag_2(\mathbf{1a})_2](O_3SCF_3)_2$ (2a). When the imine-H doublets of **2a** were observed as a function of the temperature (294–330 K), it was found that $^3J(^1H-^{107,109}Ag)$ of the imine-H(B) resonance (6.3 Hz) coalesced to a singlet at 308 K while the imine-H(A) doublet (9.3 Hz) became a singlet at 317 K. Thus, above 308 K an intermolecular Ag^+ exchange becomes visible on the NMR time scale. The fact that up to 330 K (upper temperature limit) these H(A) and H(B) singlets broaden but do not coalesce shows that imine-H(A), -H(B) site exchange is slow on the NMR time scale (250 MHz) over the whole temperature range studied. However, confirmation that the latter process does take place was proved by SST (spin saturation transfer) experiments using pure **2a**. At four different temperatures between 253 and 293 K CW ^1H irradiation of the imine-H(A) doublet (δ 8.87) resulted in a reduced intensity of the imine-H(B) doublet ($1/\tau = 0.94\ s^{-1}$ (253 K), 1.19 s^{-1} (268 K), 1.93 s^{-1} (273 K), 11.99 s^{-1} (293 K); see Experimental Section). When the values of ln $(1/\tau)$ and ln $(1/\tau T)$ were plotted vs. $1/T$, no straight lines were obtained, indicating that two (or more) reaction types with comparable rates are involved in this imine-H(A), -H(B) exchange process (see Discussion).

The influence of free Ag^+, as $[Ag(O_3SCF_3)]$, and free ligand on the two exchange processes mentioned above has been studied in separate experiments.

Complex 2a in the Presence of Added $[Ag(O_3SCF_3)]$. While the concentration of **2a** was kept constant, it was found that increase of the $[Ag(O_3SCF_3)]$ concentration resulted in a decrease of the temperature at which the loss of $^3J(^1H-^{107,109}Ag)$ on both imine-H resonances occurred. For example, at 210 K the ^1H NMR spectrum (400 MHz) of a mixture of **2a** (0.032 M) and $[Ag(O_3SCF_3)]$ (0.014 M) still showed a sharp doublet for imine H(A) (δ = 8.87) but an already broadened singlet for imine H(B) (δ = 8.69). Increasing the temperature of this solution to 213 K resulted in a coalescence of the imine-H(A) doublet, indicating that above this temperature the Ag^+ exchange was fast on the NMR time scale. A small increase of the $[Ag(O_3SCF_3)]$ concentration to 0.016 M already resulted in the observation of two sharp singlets for both imine H(A) and H(B) at 210 K, the lowest temperature at which it was possible to measure ^1H NMR spectra in methanol-d_4. It was not possible to determine by ^1H NMR the $[Ag(O_3SCF_3)]$ concentration dependency and hence the rate constant of the Ag^+ exchange process between **2a** and $[Ag(O_3SCF_3)]$. Furthermore, it was also not possible to determine whether this process depends on the concentration of **2a** because loss of $^3J(^1H-^{107,109}Ag)$ (in samples containing different concentrations of **2a** and a 0.01 M concentration of $[Ag(O_3SCF_3)]$) was only observed at temperatures close to the experimental limit.

The imine-H(A), -H(B) site-exchange process is in the slow-exchange region over the whole temperature range studied (210–305 K, 400 MHz for the (0.032 M) **2a**/(0.014 M) $[Ag(O_3SCF_3)]$ mixture, see also Figure 4B). The influence of the concentration of **2a** and $[Ag(O_3SCF_3)]$ on the imine-H(A), -H(B) exchange has been studied on a 250-MHz spectrometer by line width broadening methods (see Experimental Section) using various concentrations of **2a** (0.009–0.053 M with 0.081 M $[Ag(O_3SCF_3)]$) or of $[Ag(O_3SCF_3)]$ (0.048–0.202 M with 0.025 M **2a**). These latter experiments show that the rate of imine-H(A), -H(B) exchange is linearly dependent on the $[Ag(O_3SCF_3)]$ concen-

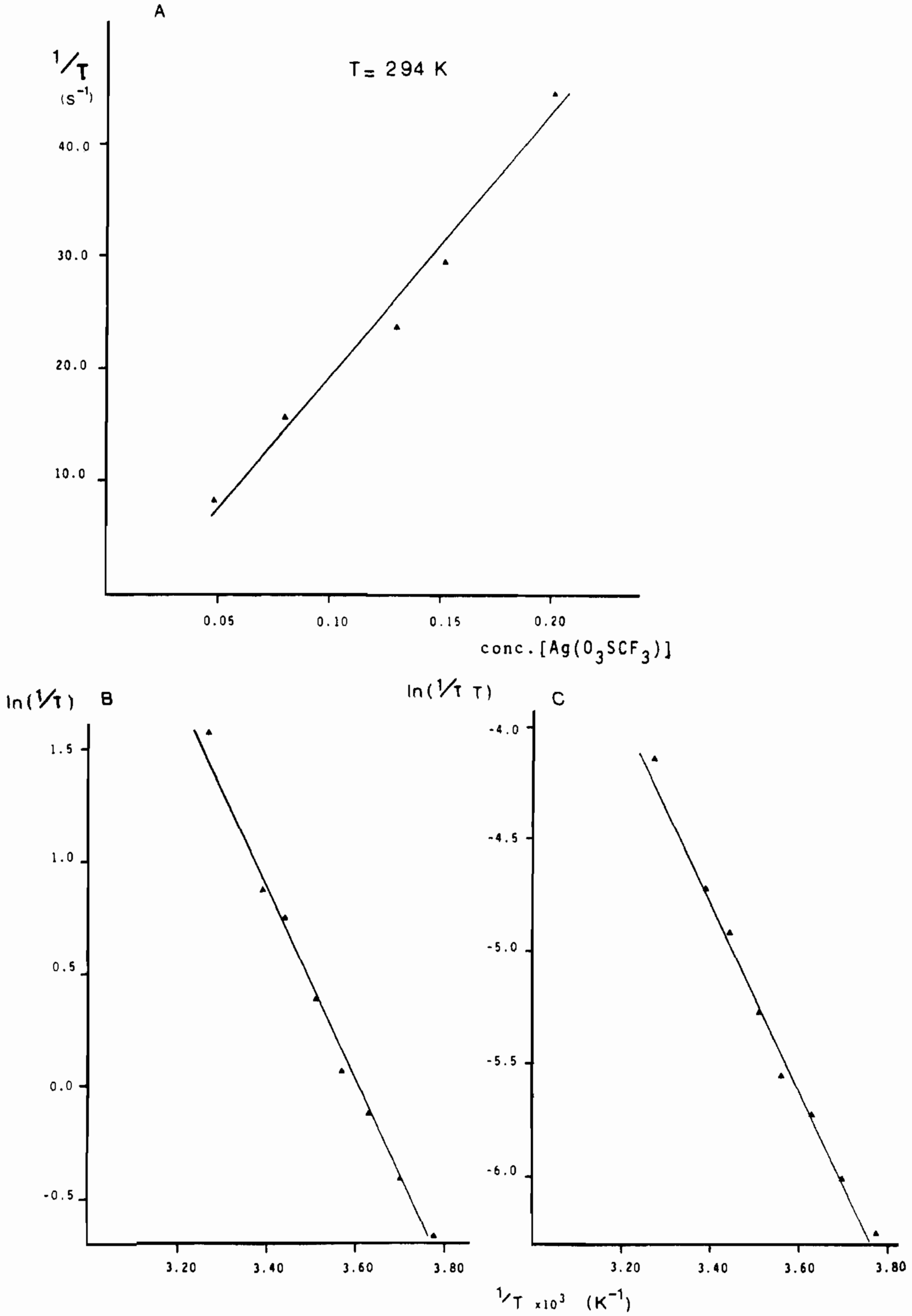

Figure 3. Plot of $1/\tau$ at 294 K (A) vs. the added [$Ag(O_3SCF_3)$] concentration in a sample of **2a** (0.025 M) and plots of ln $(1/\tau)$ vs. $1/T$ (B) and ln $(1/\tau T)$ vs. $1/T$ (C) of a sample of (0.032 M) **2a** and (0.014 M) [$Ag(O_3SCF_3)$].

tration (see Figure 3 and Table III) but independent of the concentration of [$Ag_2(\mathbf{1a})_2$]$(O_3SCF_3)_2$ (**2a**). The rate constant of the imine-H(A), -H(B) exchange process in a sample of 0.032 M **2a** and 0.014 M [$Ag(O_3SCF_3)$] was determined by a series of SST experiments at eight different temperatures in the range 265–305 K (on a 400-MHz spectrometer, see Experimental Section and Table III). For this [$Ag_2(\mathbf{1a})_2$]$(O_3SCF_3)_2$/[$Ag(O_3SCF_3)$] system the rate constant $k_y = A \exp(-E_A/RT)$ with a frequency factor $A = 7.0 \times 10^8$ and $E_A = 37.1$ kJ/mol (see Discussion). The plot of ln $(1/\tau T)$ vs. $1/T$ provides the values for the energy of activation, $\Delta G = 59.8$ kJ/mol, the enthalpy, $\Delta H = 34.7$ kJ/mol, and entropy, $\Delta S = -84$ $J/$(mol K).

From these results it is clear that two processes occur in the presence of free [$Ag(O_3SCF_3)$]: i.e., (i) an Ag^+-exchange process, which is already fast at 213 K, and (ii) an imine-H(A), -H(B) exchange, still slow at higher temperatures, which is linearly dependent on the concentration of free [$Ag(O_3SCF_3)$].

Complex 2a in the Presence of Free Ligand 1a. The ^1H NMR spectrum (250 MHz) of **2a** (0.037 M) and free ligand **1a** (0.078 M) at 294 K shows the two imine-H(A) and -H(B) resonances as doublets, due to $^3J(^1H-^{107,109}Ag)$, and one singlet

Table III. Values for the Rates $1/\tau$ of the Imine-H(A), -H(B) Site Exchange in $[Ag_2(1a)_2](O_3SCF_3)_2$ (2a) in the Presence of Free $[Ag(O_3SCF_3)]$[a]

compd	$1/\tau$, s^{-1} [b]	$(\Delta\nu)\tau$[b]	x	
2a (0.025 M) + $[Ag(O_3SCF_3)]$ (x M)	8.3	5.5	0.048	
	15.7	2.9	0.081	
	23.6	1.9	0.130	
	29.4	1.5	0.152	
	44.2	0.9	0.202	
	$1/\tau$, s^{-1} [c]	T, K	$1/\tau$, s^{-1} [c]	T, K
2a (0.032 M) + $[Ag(O_3SCF_3)]$ (0.014 M)	0.51	265	1.47	285
	0.66	270	2.12	290
	0.89	275	2.38	295
	1.07	280	4.86	305

[a] Measured in methanol-d_4. [b] Obtained by using the equation $1/\tau = (\pi/2^{1/2})(\delta\nu^2 - \delta\nu_e^2)^{1/2}$ (see Experimental Section). The error introduced in ln $(1/\tau)$ does not exceed 10% for values of $(\Delta\nu)\tau < 5$.[17] Measured on a Bruker WM 250 instrument. [c] Obtained by using SST; measured on a Bruker WM 400 instrument.

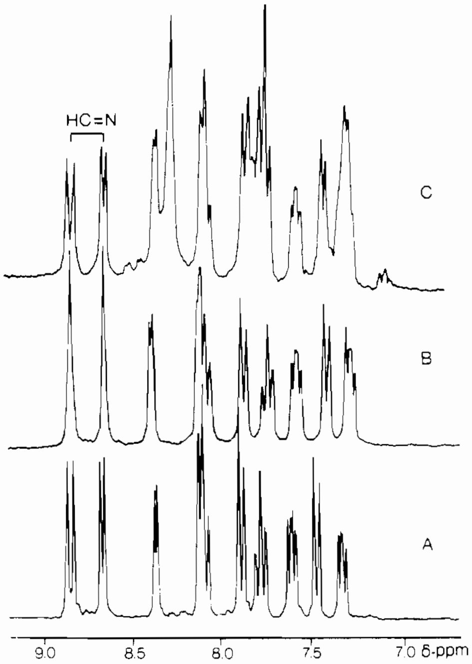

Figure 4. Aromatic part of the ^1H NMR (250 MHz) spectra at 294 K of pure $[Ag_2(1a)_2](O_3SCF_3)_2$ (**2a**) (A), of **2a** (0.032 M) with added $[Ag(O_3SCF_3)]$ (0.014 M) (B), and of **2a** (0.037 M) with free ligand **1a** (0.078 M) (C).

for the imine-H atoms of free **1a** (see Figure 4). CW ^1H irradiation of the imine-H(A) doublet of **2a** resulted in a strong reduction both of the imine-H(B) doublet and of the imine-H singlet of the free ligand. Likewise, irradiation of the imine resonance of the free ligand resulted in a decrease of intensity of both imine-H(A) and -H(B) resonances of **2a**.

These qualitative SST experiments indicate that an intermolecular exchange of coordinated and free ligands is occurring. It was not possible to determine the rate of the process and the order of the reaction by line-broadening methods because of overlap of the pyridine-H-6 resonance of site A with the imine-H signal of the free ligand. Neither could we determine the order of the reaction by SST, because of the imine-H(A), -H(B) exchange that is also taking place. From the experiments it can nevertheless be concluded that for **2a** the rate of ligand exchange is much slower than the rate of Ag^+ exchange (vide supra).

Pure $[Ag_2(1b)_2](O_3SCF_3)_2$ (2b). In the whole temperature range studied (210–330 K) the imine H atoms of the A and B sites appear as doublets due to $^3J(^1H-^{107,109}Ag)$. Irradiation of the pyridine–imine-H(A) resonances had no effect on the intensities of the corresponding H(B) signals. There is thus no evidence for H(A)–H(B) site exchange or Ag^+ exchange.

Complex 2b in the Presence of Added $[Ag(O_3SCF_3)]$. In the ^1H NMR spectra (250 MHz, 300 K) of mixtures of **2b** (0.037 M) and $[Ag(O_3SCF_3)]$ over a wide concentration range (0.079–0.334 M) neither of the imine doublet resonances changed; i.e. $^3J(^1H-^{107,109}Ag)$ values were retained. It was not possible to observe the imine-H(A), -H(B) exchange by SST experiments because of their small chemical shift difference and overlap of the resonances of the pyridine-H(A) and -H(B) atoms.

Complex 2b in the Presence of Free Ligand 1b. CW ^1H irradiation of the imine-H resonance of the free ligand **1b** (0.020 M) at 300 K (250 MHz) had no effect on the intensities of the imine-H(A) and -H(B) resonances of complex **2b** (0.037 M).

As regards exchange with $[Ag(O_3SCF_3)]$ and free ligand it may be concluded from the above results that **2b** (R = Me) is kinetically much more stable than **2a** (R = H).

$[Cu_2(1)_2](O_3SCF_3)_2$ (R = H, 3a; R = Me, 3b). The ^1H NMR spectra (250 MHz) of solutions of the pure copper(I) complexes $[Cu_2(1)_2](O_3SCF_3)_2$ (**3a,b**) as well as of solutions of these complexes with free ligands **1a** and **1b** respectively did not reveal any evidence for the occurrence of imine-H(A), -H(B) exchange reactions in the temperature range 210–330 K. Even SST experiments performed at 300 K (250 MHz) did not show the presence of imine-H(A), -H(B) exchange.

Because of the absence of $^3J(^1H-^{63,65}Cu)$ couplings on the imine-H resonances of these complexes direct information for the corresponding Cu^+-exchange reactions could not be obtained. Furthermore, NMR measurements of samples of the complexes in the presence of free Cu^+ ions were not performed because of the experimental difficulties encountered with free $[Cu(O_3SCF_3)]\cdot{}^1/_2C_6H_6$, which is very reactive in methanol-d_4.

Dynamic ^1H NMR Study in Methanol-d_4 of $[M_2(4)_2](O_3SCF_3)_2$ (4 = 1,2-(6-R-py-2-CH=N)$_2$Et; R = H (a), R = Me (b)). $[Ag_2(4)_2](O_3SCF_3)_2$ (R = H, 5a; R = Me, 5b). The ^1H NMR spectra (250 MHz) of these silver(I) complexes show at 210 K only one pyridine–imine pattern in which the imine-H resonance appears as a sharp doublet due to $^3J(^1H-^{107,109}Ag)$; for **5a** ^3J = 8.5 Hz, and for **5b** ^3J = 9.3 Hz. This observation is in accord with the INEPT ^{15}N NMR results for **5b** (vide supra). The presence of $^3J(^1H-^{107,109}Ag)$ reveals that the Ag^+ exchange is not taking place while the isochronous pyridine–imine patterns indicate that even at this temperature the exchange between sites H(A) and H(B) is fast on the NMR time scale. It was found that $^3J(^1H-^{107,109}Ag)$ on the imine-H resonance was lost at higher temperatures with coalescence of the doublet structure occurring at 241 K for **5a** and at 324 K for **5b**. Increase of Ag^+ concentrations by adding $[Ag(O_3SCF_3)]$ resulted in a decrease of these coalescence temperatures. Again it is to be noted that, for the same reasons as given for the case of **2a** with $[Ag(O_3SCF_3)]$, it was not possible to determine the order and the rate constant of this Ag^+ exchange by ^1H NMR measurements.

Pure $[Cu_2(4)_2](O_3SCF_3)_2$ (R = H, 6a; R = Me, 6b). The ^1H NMR spectra of the copper(I) complexes **6a** and **6b** show from 210 to 330 K one sharp pyridine–imine pattern, indicating that also in these copper(I) complexes with the 1,2-ethanediyl bridging groups the imine-H(A), -H(B) site exchange is fast on the NMR time scale.

Dynamic Behavior in Methanol-d_4 or CD_2Cl_2 of the Free N_4 Ligands 1 and 4. The ^1H NMR spectra of the free ligands **1a** and **1b** with the (*R,S*)-1,2-cyclohexanediyl bridging group, as well as of **4a** and **4b** having the 1,2-ethanediyl bridge, show from 190 to 330 K one pyridine–imine-H resonance pattern and either a multiplet pattern for the cyclohexanediyl groups (**1a** and **1b**) or a singlet for the four ethanediyl H atoms (**4a**

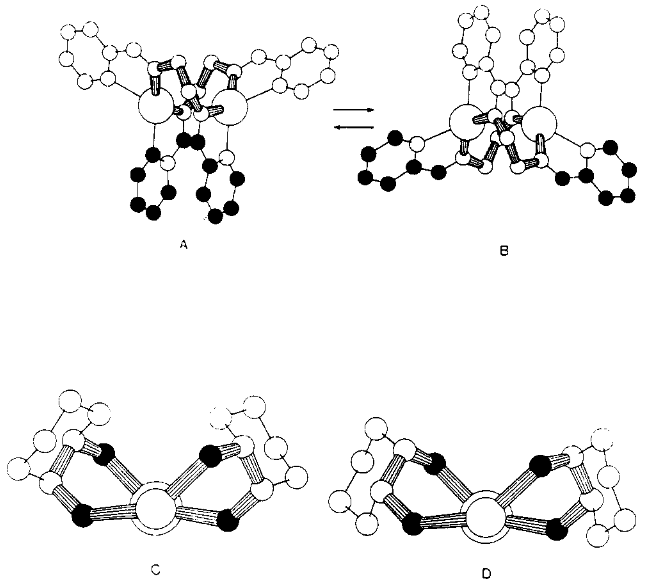

Figure 5. Representation of the conformational process in the $[M_2(\mathbf{4})_2]^{2+}$ dications (A and B) and projections down the M–M axis of the endo-$\Delta^{RS}_{SR}\Delta$ (C) and exo-$\Delta^{RS}_{SR}\Delta$ (D) forms of the $[M_2(\mathbf{1})_2]^{2+}$ dications.

and **4b**) (see Table II). ^{13}C NMR spectra also show only one pyridine–imine ^{13}C pattern even at low temperature (190 K). In the ^{13}C spectra of **1a** and **1b** six resonances are observed for the cyclohexanediyl unit at low temperature.[1] These resonances coalesce two by two to finally give three signals at 223 K (in CD_3OD or CD_2Cl_2), indicating that above this temperature a fast chair–chair conformational process is taking place on the ^{13}C NMR time scale.

Discussion

The results presented here support our earlier view[1] that the polydentate N_4 donor ligands (*R*,*S*)-1,2-(6-R-py-2-CH=N)$_2$Cy (R = H, **1a**; R = Me, **1b**) used in our studies have a strong preference for the bis-bidentate bonding mode when coordinated to metal 1B centers, and it appears that replacement of the cyclohexanediyl bridge by an ethanediyl group does not affect this preference. Depending on the ligand, interesting differences are observed, however, when the molecular dynamics of these $[M_2(N_4)_2]^{2+}$ dications are studied in solution. It appears that intra- and intermolecular exchange reactions involving these dications are dependent on the nature of the bridging groups as well as on the type of substituents present in the 6-positions of the py(2-CH=N) rings. Before the conclusions that can be drawn from the NMR studies may be discussed, it is necessary to outline the molecular geometry of the $[M_2(N_4)_2]^{2+}$ dications.

Conformational and Configurational Aspects of the $[M_2(N_4)_2]^{2+}$ Dications. The basic framework of the $[M_2(N_4)_2]^{2+}$ dications is a 10-membered M–N–C–C–N–M–N–C–C–N ring that results from the N(imine)–M coordination mode. The characteristic stereochemistry of this ring system is a consequence of the bis-bidentate chelation of the N_4 ligands in combination with the pseudotetrahedral geometries of the metal 1B centers. The molecular geometry of $[Ag_2(\mathbf{1a})_2]^{2+}$ in the solid (Figure 1) shows that the 10-membered ring has a $\delta\delta$[19] conformation. A representation of the $[M_2(\mathbf{4})_2]^{2+}$ dication with the ethanediyl bridge is presented in Figure 5A. To each of the imine-N atoms in the 10-membered ring is attached a 2-pyridine group, which also coordinates to the M atoms, resulting in chelate-bonded pyridine–imine units.

In combination with the $\delta\delta$ (or $\lambda\lambda$) conformation[20] of the 10-membered ring both metal centers in these $[M_2(N_4)]^{2+}$ dications have $\Delta\Delta$ (or $\Lambda\Lambda$)[19] configurations. In principle structures in which the metal centers also have opposite configurations (i.e. $\Delta\Lambda$) are feasible. However, study of molecular models shows that the constraints imposed by the vicinal interactions along the N–C–C–N bonds in the bridging groups makes these $\Delta\Lambda$ isomers less favorable than the $\Delta\Delta$ and $\Lambda\Lambda$ ones.

Figure 5 clearly shows that the structure of $[M_2(\mathbf{4a})_2]^{2+}$ contains two different types of pyridine–imine moieties. For our NMR discussion it is important to realize that these pyridine–imine moieties can interchange environments as a result of a fluxional process of the molecular framework in which Ag–N bond dissociation does not take place. In the case of the $[M_2(\mathbf{4})_2]^{2+}$ dications containing the CH_2CH_2 bridges this movement always produces stereochemically identical structures, leaving the conformation of the 10-membered ring ($\delta\delta$ or $\lambda\lambda$) as well as the configuration of the M^+ centers ($\Delta\Delta$ or $\Lambda\Lambda$) unaffected (see Figure 5A,B).

When chiral C atoms are introduced into the C_2 bridges, the number of possible stereoisomers is greatly increased. This discussion will be restricted to the $[M_2(\mathbf{1})_2]^{2+}$ dications containing the (*R*,*S*)-1,2-cyclohexanediyl bridges.

For reasons outlined above, the M^+ centers here will again have the same configurations, i.e. $\Delta\Delta$ or $\Lambda\Lambda$. However, the (*R*,*S*)-C_2 bridges can be positioned between the M^+ centers such that C atoms of either equivalent or opposite configurations are facing these centers. This produces stereoisomers, which can be denoted, for instance in the case that the metal centers have $\Delta\Delta$ configurations, as $\Delta^{RS}_{RS}\Delta$ and $\Delta^{RS}_{SR}\Delta$ (a complex illustrative of the latter notation is the dication of **2a** as shown in Figure 1). In the $\Delta^{RS}_{RS}\Delta$ stereoisomer a fluxional process may take place as has been discussed for the $[M_2(\mathbf{4})_2]^{2+}$ dications, between two stereochemically equivalent structures. In the case of the $\Delta^{RS}_{SR}\Delta$ stereoisomer, however, this fluxional process occurs between nonidentical molecules as a consequence of the difference in the relative positioning of the cyclohexanediyl rings with respect to the 10-membered M–N–C–C–N–M–N–C–C–N ring. These stereoisomers can be denoted for example as endo-$\Delta^{RS}_{SR}\Delta$ in Figure 5C and exo-$\Delta^{RS}_{SR}\Delta$ in Figure 5D.

Dynamic Behavior of the $[M_2(\mathbf{4})_2]^{2+}$ and $[M_2(\mathbf{1})_2]^{2+}$ Dications in Solution. The fact that at 210 K one ligand resonance pattern is observed for $[M_2(\mathbf{4})_2]^{2+}$ indicates that the intramolecular imine-H(A), -H(B) exchange, i.e. the process shown in Figure 5, is in the fast exchange even at this temperature. For the following discussion it is important to recall that this movement occurs between two identical states of the $[M_2(\mathbf{4})_2]^{2+}$ dications.

The coupling constants $^3J(^1H-^{107,109}Ag)$ and $^1J(^{15}N-^{107,109}Ag)$ are very sensitive probes for the detection of processes involving intermolecular Ag^+ exchange, because the occurrence of such processes would lead to disappearance of these couplings. In the case of $[Ag_2(\mathbf{4a})_2]^{2+}$ elevated temperatures as well as the addition of small amounts of $[Ag(O_3SCF_3)]$ cause coalescence of, e.g., the doublet imine-H resonance, as $^3J(^1H-^{107,109}Ag)$ is lost. Introduction of a methyl group in the 6-position of the pyridine rings increases the stability of the

---

[19] For the abbreviations of δ, λ, and Δ, Λ: Ernst, R. E.; O'Connor, M. J.; Holm, R. H. *J. Am. Chem. Soc.* **1967**, *89*, 6104. "IUPAC Nomenclature of Inorganic Chemistry"; Butterworths: London, 1970; p 80.

[20] Molecular models show that the C_2 bridges in the $[M_2(N_4)_2]^{2+}$ dications have $\delta\delta$(C,C) conformations (relative to the Ag···Ag axis) (see Figure 5A) in combination with $\Delta\Delta$ configurations of the metal centers (or $\Lambda\Lambda\lambda\lambda$(C,C)). However, diastereomeric structures denoted $\Delta\Delta\lambda\lambda$(C,C) or $\Lambda\Lambda\delta\delta$(C,C) may likewise exist. Our NMR results indicate that either the two diastereoisomers are in a fast exchange or one of the diastereoisomers has a much higher stability. We therefore omit this distinction between the $\delta\delta$(C,C) and $\lambda\lambda$(C,C) conformers.

dication with regard to intermolecular processes involving Ag^+ exchange: the T_{coal} of the $^3J(^1H-^{107,109}Ag)$ value of the 6-methyl product $[Ag_2(\mathbf{4b})_2]^{2+}$ lies 84 K above that of the corresponding $[Ag_2(\mathbf{4a})_2]^{2+}$ dication. A possible explanation is given below in the discussion of the $[M_2(\mathbf{1})_2]^{2+}$ dications.

The NMR spectra of the corresponding Cu(I) complexes $[Cu_2(\mathbf{4})_2](O_3SCF_3)_2$ lack this coupling information. However, recent work by us[21] shows that the copper(I) species are in general more stable toward Cu^+ exchange than the silver(I) complexes toward Ag^+ exchange.

A different situation is met when the dynamic behavior of the dications $[M_2(\mathbf{1})_2]^{2+}$ containing the (*R*,*S*)-1,2-cyclohexanediyl bridges is discussed. Again it is the NMR data gathered for the $[Ag_2(\mathbf{1})_2](O_3SCF_3)_2$ complexes that give us extensive information concerning both the nature of the pure complexes and the occurrence of inter- and intramolecular processes in solution.

On the basis of the available ^{109}Ag NMR data it can be concluded that in solution the $[Ag_2(\mathbf{1})_2]^{2+}$ dications exist exclusively in the $\Delta^{RS}_{SR}\Delta$ (or its enantiomeric) diastereomeric form. In the case of the alternative isomer, $\Delta^{RS}_{RS}\Delta$ and its enantiomer $\Lambda^{SR}_{SR}\Lambda$, one expects to see in the slow exchange four pyridine–imine-H patterns and two ^{109}Ag resonances. A fluxional movement of the type described above (see Figure 5), in this case between two identical structures, would result in coalescence of the four ^1H patterns into two. However, such movement would still leave the two ^{109}Ag resonances unaffected because the diastereotopic environments are not interchanged by this process. Yet in practice one only observes one ^{109}Ag resonance in the spectra of **2a** and **2b**. The possibility of accidentally coincident resonances can be excluded in view of the high sensitivity of $\delta(^{109}Ag)$ for even small structural changes,[21] and we, therefore, conclude that the $\Delta^{RS}_{RS}\Delta$ and $\Lambda^{SR}_{SR}\Lambda$ forms are not present in solution.

Figure 5C,D shows the fluxional movement for the endo- and exo-$\Delta^{RS}_{SR}\Delta$ conformers, which are diastereoisomers and can therefore be distinguished by NMR. It is, however, very unlikely that they are equally populated. The fact that we observe in the ^1H and ^{15}N NMR spectra patterns that are indicative of only one diastereoisomer can be explained by either (i) a large preference for one diastereoisomer, most likely endo-$\Delta^{RS}_{SR}\Delta$ and its enantiomer or (ii) a rapid interchange between the two conformers as illustrated in Figure 5C,D. The latter possibility is in line with the observed multiplicity of the patterns found in the spectra. However, the large differences in $^{107,109}Ag$ couplings on the two imine ^1H signals and on the imine-^{15}N and pyridine-^{15}N resonances are not in agreement with such a rapid interchange between the endo and exo conformers. Accordingly, it may be concluded that in solution the $[M_2(\mathbf{1})_2]^{2+}$ dications exist primarily as the endo-$\Delta^{RS}_{SR}\Delta$ form (as shown in Figure 1) and its enantiomer endo-$\Lambda^{SR}_{RS}\Lambda$.

Mechanistic Aspects of the Exchange Processes in the $[Ag_2(\mathbf{1})_2]^{2+}$ Dications. Imine-H(A), -H(B) site exchange in the ^1H NMR spectra of $[Ag_2(\mathbf{1a})_2](O_3SCF_3)_2$ (**2a**) indicates that an interconversion process is occurring between the two enantiomers, $\Delta^{RS}_{SR}\Delta$ and $\Lambda^{SR}_{RS}\Lambda$. To achieve imine-H(A), -H(B) site exchange in these molecules, this interconversion must involve Ag–N bond dissociation and inversion of the configuration of both Ag(I) centers (the ΔΛ configuration of the dication is unstable, vide supra). The rate of this process is slow compared to the H(A)–H(B) exchange observed in the $[M_2(\mathbf{4})_2]^{2+}$ dications (Figure 5A,B).

In the $[Ag_2(\mathbf{1a})_2]^{2+}$ dication various possible reaction pathways leading to imine-H(A), -H(B) exchange, which do not involve intermolecular Ag^+- or ligand-exchange processes, can be considered. First, N(pyridine)–Ag bond dissociation may occur leading to a change of the tetrahedral coordination geometry into a trigonal-planar one around both Ag(I) centers. Second, such N(pyridine)–Ag bond dissociations may take place, resulting in linear coordination geometries in which the metal 1B sites are primarily coordinated to the imine-*N* atoms. This situation is very much like the linear N–Ag–N coordination observed in the stable dications $[Ag_2(N_2S_2)_2]^{2+}$ (N_2S_2 = (*R*,*S*)-1,2-(5-R-thiophene-2-CH=N)$_2$Cy (R = H, Me)).[22] In both cases re-formation of the N(pyridine)–Ag bonds can then occur with either retention or inversion of configuration of the Ag(I) center. However, the ^1H NMR data for the $[Ag_2(\mathbf{1})_2]^{2+}$ dications show that this imine-H(A), -H(B) exchange only takes place when intermolecular Ag^+- or ligand-exchange processes also occur. Therefore it may be concluded that imine-H(A), -H(B) exchange without intermolecular Ag^+ or ligand exchange (see above) has high-energy pathways.

From the ^1H NMR experiments using pure $[Ag_2(\mathbf{1a})_2](O_3SCF_3)_2$ (**2a**) and **2a** in the presence of $[Ag(O_3SCF_3)]$ it is clear than an intermolecular Ag^+ exchange, evidenced by the loss of $^3J(^1H-^{107,109}Ag)$ on the imine-H resonances, is taking place. A possible mechanism for this Ag^+ exchange involves a solvent- or anion $(O_3SCF_3^-)$-assisted dissociation of one Ag^+ center via Ag–N bond rupturing at one pyridine–imine end of each of the **1a** ligands. In the reverse reaction an external Ag^+ ion can attack the empty place in the $[Ag(\mathbf{1a})_2]^+$ species. This process, which leads to a loss of $^3J(^1H-^{107,109}Ag)$, is presented in eq 1.

$$[Ag_2(\mathbf{1a})_2]^{2+} \underset{-1}{\overset{1}{\rightleftharpoons}} [Ag(\mathbf{1a})_2]^+ + Ag^+ \qquad (1)$$

A second possible mechanism involves dissociation of a N(pyridine) site from one Ag(I) center of the $[Ag_2(\mathbf{1a})_2]^{2+}$ dication, followed by attack and association at this site of an external Ag′, which may be either a $[Ag(O_3SCF_3)]$ molecule or a solvated Ag^+ ion. In the following stage the incoming silver(I) replaces the parent Ag^+ center. The overall result, as shown by eq 2, is Ag^+ exchange.

$$[Ag(\mathbf{1a})Ag(\mathbf{1a})]^{2+} + Ag'^{*} \underset{-2}{\overset{2}{\rightleftharpoons}}$$
$$[AgAg'^{*}(\mathbf{1a})Ag(\mathbf{1a})]^{2+} \underset{2}{\overset{-2}{\rightleftharpoons}} [Ag^{*}(\mathbf{1a})Ag(\mathbf{1a})]^{2+} + Ag' \qquad (2)$$

The SST experiments show qualitatively that ligand exchange takes place in samples containing **2a** in the presence of free N_4 ligand. This may proceed either via a dissociative mechanism (eq 3) or via a direct bimolecular reaction, between

$$[Ag_2(\mathbf{1a})_2]^{2+} \underset{-3}{\overset{3}{\rightleftharpoons}} [Ag_2(\mathbf{1a})]^{2+} + \mathbf{1a} \qquad (3)$$

the N_4 ligand, **1a**, and complex **2a** (eq 4). From the ^1H NMR

$$[Ag_2(\mathbf{1a})_2]^{2+} + \mathbf{1a}^{*} \underset{-4}{\overset{4}{\rightleftharpoons}} [Ag_2(\mathbf{1a}\mathbf{1a}^{*})]^{2+} + \mathbf{1a} \qquad (4)$$

results it was not possible to determine which of these two mechanisms is operative, though it is clear that the intermolecular ligand-exchange process is very much slower than Ag^+ exchange and will therefore not be discussed further.

What are the possible reaction pathways leading to imine-H(A), -H(B) exchange induced by the intermolecular Ag^+ exchange? When Ag^+ exchange takes place via the dissociative mechanism (eq 1) the mononuclear $[Ag(\mathbf{1a})_2]^+$ cation

---

[21] van Stein, G. C.; van Koten, G.; Vrieze, K.; de Bok, B.; Taylor, L. C.; Brevard, C. *Inorg. Chim. Acta* **1984**, *89*, 29. van Stein, G. C.; van Koten, G.; Brevard, C. *J. Organomet. Chem.* **1982**, *226*, C27.

[22] van Stein, G. C.; van Koten, G.; Blank, F.; Taylor, L. C.; Vrieze, K.; Spek, A. L.; Brevard, C. *Inorg. Chem.*, in press. van Stein, G. C.; van Koten, G.; Vrieze, K.; Spek, A. L.; Klop, E. A.; Brevard, C. *Inorg. Chim. Acta*, in press.

Scheme I

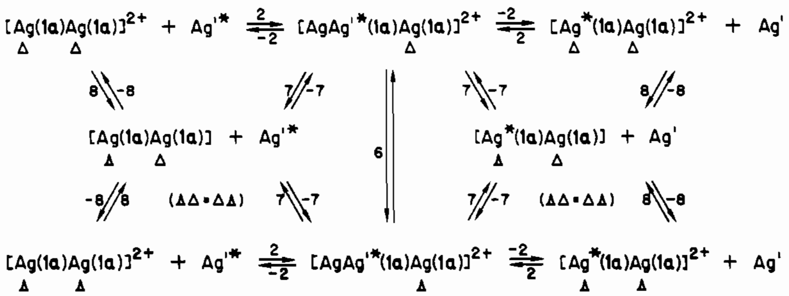

is formed reversibly. The single metal 1B center in this monocation is now coordinated either by (i) two chelating pyridine–imine units as in $[\mathrm{Ag(py\text{-}2\text{-}CH{=}N{-}R)_2}]^{+}$[21] or by (ii) a set of imine-N-donor atoms, a situation we have previously observed for the $[\mathrm{Ag(N_2S_2)_2}](\mathrm{O_3SCF_3})$ complexes.[18] In these proposed intermediates of (i) and (ii) inversion of configuration of the metal center (cf. eq 5) can take place.[21,22]

$$\underset{\Delta\Delta}{[\mathrm{Ag_2}(\mathbf{1a})_2]^{2+}} \underset{-1}{\overset{1}{\rightleftharpoons}} \underset{\Delta}{[\mathrm{Ag}(\mathbf{1a})_2]^{+}} + \mathrm{Ag}' \underset{-5}{\overset{5}{\rightleftharpoons}} \underset{\Lambda}{[\mathrm{Ag}(\mathbf{1a})_2]^{+}} + \mathrm{Ag}' \underset{1}{\overset{-1}{\rightleftharpoons}} \underset{\Lambda\Lambda}{[\mathrm{Ag_2}(\mathbf{1a})_2]^{2+}} \quad (5)$$

When the second $\mathrm{Ag^+}$ ion is taken up again by the $[\mathrm{Ag}(\mathbf{1a})_2]^+$ cation, the 1/1 $[\mathrm{Ag_2}(\mathbf{1a})_2]^{2+}$ dication with either ΔΔ or ΛΛ configurations at the $\mathrm{Ag^+}$ centers is re-formed. When inversion of configuration occurs, this is observed as imine-H(A), -H(B) exchange in the ^{1}H NMR spectra.

When $\mathrm{Ag^+}$ exchange occurs according to eq 2 Ag′ ($[\mathrm{Ag(O_3SCF_3)}]$ or $\mathrm{Ag^+}$) attacks an uncoordinated N(pyridine) site to form a new Ag–N(pyridine) bond and subsequently a new Ag–N(imine) bond may be formed, thus leading to the $[\mathrm{AgAg'}(\mathbf{1a})\text{–}\mathrm{Ag}(\mathbf{1a})]^{2+}$ species in Scheme I. In further ligand dissociation–association steps this process may lead to silver(I) exchange, which can take place either with retention of configuration of the metal center at the reaction side of the dication (i.e. ΔΔ and ΛΛ are re-formed) or with inversion of the particular metal center leading to the formation of the less stable ΔΛ structure (vide supra).

It is important to recall that for the imine-H(A), -H(B) exchange process inversion of configuration at both Ag centers, i.e. a ΔΔ–ΛΛ overall inversion, is required. This can occur by starting either from the $[\mathrm{AgAg'^*}(\mathbf{1a})\mathrm{Ag}(\mathbf{1a})]^{2+}$ species (via process 6), which are then real intermediates, or from the ΛΔ (ΔΛ) structures (via processes 7 and −8). In both cases the required inversion of configuration at the other side of the intermediate can be accomplished by Ag–N(pyridine) bond dissociation. This as we have seen generates a three-coordinated Ag(I) center, and re-formation of the Ag–N(pyridine) bond can occur with either retention or inversion of the configuration of this Ag(I) center. The feasibility of such a process occurring is shown by the result of a recent investigation of the dynamic behavior of $[\mathrm{Ag(6\text{-}R\text{-}py\text{-}2\text{-}CH{=}N{-}R')_2}]^+$ cations.[21]

An equation for the rate, $1/\tau$, of the imine-H(A), -H(B) exchange, which is induced by intermolecular $\mathrm{Ag^+}$ exchange, can be set up as shown by eq 9,

$$1/\tau = k_x + k_y[\mathrm{Ag(O_3SCF_3)}] \qquad (9)$$

in which k_x represents the rate of the imine H(A), -H(B) exchange step represented in eq 5 (dissociative mechanism) and k_y the one in the exchange according to Scheme I (associative mechanism).

From the fact that we did not obtain straight lines when plotting $1/\tau$ and $1/\tau T$ vs. $1/T$ for the *pure* complex **2a**, it is clear that in this case the $\mathrm{Ag^+}$ and the imine-H(A), -H(B) exchange proceeds via two pathways probably involving both the dissociative (cf. eq 5) and the associative mechanism (cf. Scheme I).

The ^{1}H NMR results obtained for samples of **2a** with free $[\mathrm{Ag(O_3SCF_3)}]$ show that the rate of imine-H(A), -H(B) exchange ($1/\tau$) in these samples is linearly dependent on the concentration of free $[\mathrm{Ag(O_3SCF_3)}]$. Furthermore, straight lines were also obtained in the ln ($1/\tau$) and ln ($1/\tau T$) vs. $1/T$ plots (see Figure 3B,C) of the sample containing 0.032 M of **2a** and additional 0.014 M of $[\mathrm{Ag(O_3SCF_3)}]$. These results indicate that in samples containing **2a** in the presence of $[\mathrm{Ag(O_3SCF_3)}]$ the imine-H(A), -H(B) exchange process of eq 5 is unimportant (i.e. k_x in eq 9 is negligible) compared to the process(es) of Scheme I. The process outlined in Scheme I shows that several routes can lead to overall inversion of configuration at the metal 1B centers (i.e. steps 6–8 or their reverse[23]). The value for E_A (37.1 kJ/mol) as obtained by SST for the sample of 0.032 M **2a** and 0.014 M $[\mathrm{Ag(O_3SCF_3)}]$ indicates that this imine-H(A), -H(B) exchange, induced by $\mathrm{Ag^+}$ exchange (step 2), is following a low-energy pathway, whereas the small value for the frequency factor A (7.0×10^8) shows that this exchange proceeds via a specific pathway.

In the $[\mathrm{Ag_2(N_4)_2}]^{2+}$ ions the introduction of methyl groups on the 6-positions of the 2-CH=Npy rings in the ligand skeleton has a large effect on the rate of $\mathrm{Ag^+}$ exchange. This is reflected by the difference in temperatures at which the $^3J(^1\mathrm{H}\text{–}^{107,109}\mathrm{Ag})$ couplings on the imine-H resonances disappear in the $[\mathrm{Ag_2}(\mathbf{4})_2]^{2+}$ dications and by the fact that the $\mathrm{Ag^+}$ exchange in $[\mathrm{Ag_2}(\mathbf{1b})_2]^{2+}$ is in the slow-exchange limit up to 305 K (SST). A likely explanation is that the presence of Me groups on positions neighboring the dissociated pyridine N sites hinders the attack of external silver(I) on these sites, thus hindering the first step in the $\mathrm{Ag^+}$-exchange process. Furthermore, the comparison of the much slower $\mathrm{Ag^+}$ exchange in $[\mathrm{Ag_2}(\mathbf{1})_2]^{2+}$ with that in $[\mathrm{Ag_2}(\mathbf{4})_2]^{2+}$ suggests that the cyclohexanediyl groups have a further shielding effect on the sites of the dication of which silver(I) from the solution will attack.

The difference in dynamic behavior between the silver(I) complex **2a** and the copper(I) complex **3a** can be accounted for by the difference in group 1B metal–N bond strength. It is known for $[\mathrm{M(6\text{-}R\text{-}py\text{-}2\text{-}CH{=}N{-}R')_2}](\mathrm{O_3SCF_3})$ that the Ag–N bonds are very much weaker than those in the Cu complexes.[21] Moreover because of the smaller ionic radius of the copper(I) centers, the latter ions will fit better into the pyridine–imine bidentates. This will cause a contraction of the molecular structure of the $[\mathrm{M_2(N_4)_2}]^{2+}$ species, an effect that has been demonstrated in a recent study of the $[\mathrm{M(N_2S_2)_2}]^+$ cations (M = Ag(I), Cu(I)).[18]

Conclusions

The silver(I) and copper(I) complexes with the neutral $\mathrm{N_4}$ donor ligands $\mathrm{1,2\text{-}(6\text{-}R\text{-}py\text{-}2\text{-}CH{=}N)_2Et}$ (R = H, Me) have in solution as well as the solid state similar $[\mathrm{M_2(N_4)_2}](\mathrm{O_3SCF_3})_2$ structures that are analogous to those re-

---

[23] In Scheme I, step 8 involves inversion of configuration without $\mathrm{Ag^+}$ exchange and thus has a high-energy pathway. Therefore, it is less likely that the imine-H(A), -H(B) exchange will proceed via this route.

ported before for the complexes with the N_4 ligands (*R*,*S*)-1,2-(6-R-py-2-CH=N)$_2$Cy. The $[M_2(N_4)_2]^{2+}$ dications have a twofold axial symmetry. The two metal 1B centers have pseudotetrahedral geometries with similar configurations (ΔΔ or ΛΛ). The ligands, acting as bis-bidentates, contain two inequivalent pyridine–imine moieties, of which the protons may be denoted H(A) and H(B).

In solutions of the complexes having the 1,2-ethanediyl bridges H(A)–H(B) exchange is observed (on the basis of ^1H and ^{15}N NMR spectra), a process which is caused by a conformational movement between two identical structures. Furthermore, only for the silver(I) complexes could it be deduced (from loss of $^3J(^1H-^{107,109}Ag)$) that these complexes are prone to intermolecular Ag^+ exchange (above 241 K for 6-R = H and 324 K for 6-R = Me).

When chiral C atoms are introduced in the 1,2-alkanediyl bridges (N_4 = (*R*,*S*)-1,2-(6-R-py-2-CH=N)$_2$Cy), the conformational movement, now between diastereomeric structures, does not take place, because of a slightly higher stability of one of the isomers. Only in the silver(I) complex with 6-R = H could the occurrence of Ag^+ exchange be observed. This process induced a configurational ($\Delta\Delta \rightleftarrows \Lambda\Lambda$) interconversion, which was observed as H(A)–H(B) exchange. The copper(I) complexes (6-R = H, Me) and the silver(I) complex (6-R = Me) are kinetically much more stable. From dynamic ^1H NMR experiments mechanisms are proposed for the intermolecular Ag^+ exchange and the induced H(A)–H(B) exchange in the silver(I) complex with 6-R = H. It appeared that in the pure complex these processes follow both an associative and a dissociative path, while in samples of this complex and added $[Ag(O_3SCF_3)]$ the associative mechanism is dominating.

The bulkiness of the 6-R substituents and of the 1,2-alkanediyl bridges has a large influence, by a shielding effect, on the rate of intermolecular Ag^+ exchange and therefore on the rate of the configurational, ΔΔ–ΛΛ, exchange process. These rates are much lower when 6-R = Me instead of 6-R = H and when the bridging groups are (*R*,*S*)-1,2-cyclohexanediyl instead of 1,2-ethanediyl.

Intermolecular Ag^+ exchange observed in the silver(I) complexes having the ethanediyl (R = H or Me) or (*R*,*S*)-1,2-cyclohexanediyl (R = H) groups and added $[Ag(O_3SCF_3)]$ is much faster than intermolecular ligand exchange between the $[Ag_2(N_4)_2]^{2+}$ dications and free added ligand.

This study gives a view of all inter- and intramolecular processes in these binuclear $[M_2(N_4)_2]^{2+}$ dications and shows that these depend on the metal 1B center (M = Ag(I), Cu(I)) and the various substituents in the N_4 ligand system. These results may have importance in understanding the occurrence of such processes not only in coordination complexes but also in biological systems that contain metal ions in the active sites.

Acknowledgment. The FD mass spectral data were kindly collected by Prof. N. M. M. Nibbering and his co-workers. J. M. Ernsting is thanked for recording the 250-MHz ^1H NMR spectra and Dr. A. Pagelot for recording the 400-MHz ^1H NMR spectra.

Registry No. **2a**, 76317-71-0; **2b**, 76317-73-2; **3a**, 76317-75-4; **3b**, 90605-91-7; **5a**, 92346-69-5; **5b**, 92346-71-9; **6a**, 92346-73-1; **6b**, 92365-89-4.

Supplementary Material Available: Tables of IR data (Table SI) and FD mass spectral data (Table SII) of $[M_2(\mathbf{4})_2](O_3SCF_3)_2$ (M = Ag(I) or Cu(I)) (2 pages). Ordering information is given on any current masthead page.

Contribution from the Laboratoire de Physique Expérimentale B5, University of Liège, B-4000 Liège, Belgium,
Commission of the European Communities, European Institute for Transuranium Elements, D-7500 Karlsruhe, West Germany,
and Laboratoire de Chimie Analytique et de Radiochimie B6, University of Liège, B-4000 Liège, Belgium

Structural Characterization of a Terbium(III) Complex with 1,4,8,11-Tetraazacyclotetradecane-1,4,8,11-tetraacetic Acid. Lanthanide Ions and the Conformation of the 14-Membered Macrocycles

MARIE-ROSE SPIRLET,*[1] JEAN REBIZANT,[2] MARIE-FRANCE LONCIN,[3] and JEAN F. DESREUX*[3]

Received February 27, 1984

The molecular and crystal structure of $Na^+[TbTETA]^-\cdot 6H_2O\cdot {}^1/_2NaCl$ (TETA = 1,4,8,11-tetraazacyclotetradecane-1,4,8,11-tetraacetic acid) has been determined from three-dimensional X-ray intensity data. The space group is $P2/c$, and the lattice parameters are a = 17.980 (3) Å, b = 9.081 (2) Å, c = 17.713 (3) Å, β = 106.00 (1)°, and d = 1.775 g cm^{-3} for Z = 4. The structure was solved by direct methods. Full-matrix least-squares refinement with all non-hydrogen atoms treated anisotropically gave an agreement factor R of 0.036 for 4111 unique reflections. The Tb^{3+} ion is eight-coordinated, being linked to the four nitrogen atoms and the four carboxylic oxygen atoms of the ligand. The coordination polyhedron of the terbium ion is a strongly distorted dodecahedron, but although no symmetry is imposed by the space group, the TETA ligand approximates the C_2 symmetry fairly well. The conformation of the 14-membered macrocyclic ring is compared with the various conformations adopted by other macrocycles with the same cavity size. The TETA ligand exhibits a biangular {77} structure, which is the most suited for the complexation of a 4f metal ion located out of the mean plane of the macrocyclic ring. In the crystal, the $[TbTETA]^-$ complex units are associated through sodium ions and water molecules into layers that alternate with aqueous layers containing the chloride ions.

Introduction

It has long been recognized that lanthanide ions form essentially electrostatic, nondirectional coordination bonds. The lanthanide complexes are thus highly labile and exhibit a variety of structures in solution. The resulting intramolecular conformational processes are usually too fast to be observed by NMR.[4] One obvious way to find exceptions to this general rule involves the synthesis of complexes with rigid and sterically demanding ligands. The macrocyclic 1,4,7,10-tetraazacyclo-

---

(1) Laboratorire de Physique Expérimentale B5, University of Liège.
(2) European Institute for Transuranium Elements.
(3) Laboratoire de Chimie Analytique et de Radiochimie B6, University of Liège.

(4) Williams, R. J. P. *Struct. Bonding (Berlin)* **1982**, *50*, 79.

0020-1669/84/1323-4278$01.50/0